

Journal Pre-proof



Perfusion microbioreactor for CAR-Treg manufacturing

William Edwards, Ningjia Sun, Yikai Wang, Yuhan Lu, Cong Wang, Daniela Mastronicola, Cristiano Scottà, Marco Romano, Cesare M. Cejas, Antoine Espinet, Giovanna Lombardi, Ciro Chiappini

PII: S2589-0042(26)00621-8

DOI: <https://doi.org/10.1016/j.isci.2026.115246>

Reference: ISCI 115246

To appear in: *iScience*

Received Date: 16 April 2025

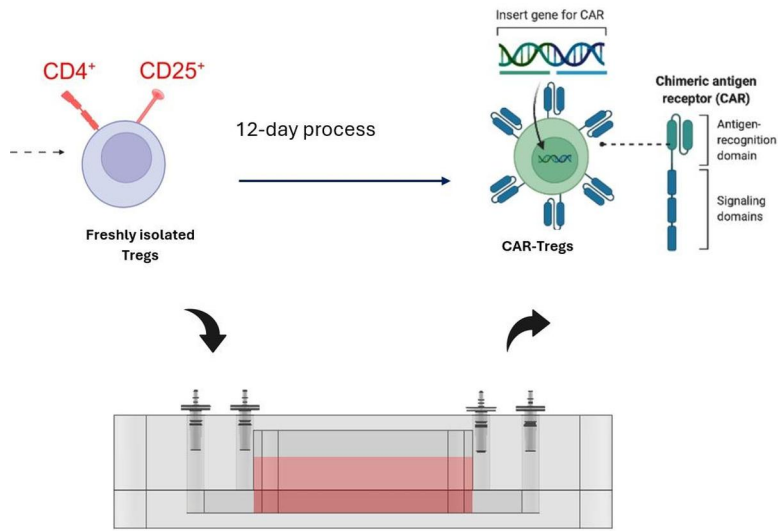
Revised Date: 10 December 2025

Accepted Date: 2 March 2026

Please cite this article as: Edwards, W., Sun, N., Wang, Y., Lu, Y., Wang, C., Mastronicola, D., Scottà, C., Romano, M., Cejas, C.M., Espinet, A., Lombardi, G., Chiappini, C., Perfusion microbioreactor for CAR-Treg manufacturing, *iScience* (2026), doi: <https://doi.org/10.1016/j.isci.2026.115246>.

This is a PDF of an article that has undergone enhancements after acceptance, such as the addition of a cover page and metadata, and formatting for readability. This version will undergo additional copyediting, typesetting and review before it is published in its final form. As such, this version is no longer the Accepted Manuscript, but it is not yet the definitive Version of Record; we are providing this early version to give early visibility of the article. Please note that Elsevier's sharing policy for the Published Journal Article applies to this version, see: <https://www.elsevier.com/about/policies-and-standards/sharing#4-published-journal-article>. Please also note that, during the production process, errors may be discovered which could affect the content, and all legal disclaimers that apply to the journal pertain.

© 2026 The Author(s). Published by Elsevier Inc.



**CLOSED-SYSTEM PERFUSION
MICROBIOREACTOR**

Journal Pre-proof

1 Perfusion microbioreactor for CAR-Treg manufacturing

2 Author list and affiliations

3 William Edwards¹ (will.j.edwards@hotmail.co.uk), Ningjia Sun¹
4 (ningjia.sun@kcl.ac.uk), Yikai Wang^{1,2} (yikai.1.wang@kcl.ac.uk), Yuhan Lu^{1,3}
5 (yuhan.1.lu@kcl.ac.uk), Cong Wang^{1,2,4} (cong.wang@kcl.ac.uk), Daniela
6 Mastronicola⁵ (daniela.mastronicola1@gstt.nhs.uk), Cristiano Scottà^{5,6}
7 (Cristiano.Scotta@brunel.ac.uk), Marco Romano⁵ (marco.romano@kcl.ac.uk),
8 Cesare M. Cejas⁷ (cesare@mfX.bio), Antoine Espinet⁷ (antoine@mfX.bio), Giovanna
9 Lombardi⁵ (giovanna.lombardi@kcl.ac.uk), ¹Ciro Chiappini^{1,2}
10 (ciro.chiappini@kcl.ac.uk, Corresponding Author and Lead Contact)

11 1 Centre for Craniofacial and Regenerative Biology, King's College London, London
12 SE1 9RT, UK

13 2 London Centre for Nanotechnology, King's College London, London WC2R 2LS, UK

14 3 Department of Bioengineering, Imperial College London, London SW7 2AZ, UK

15 4 Wenzhou Eye Valley Innovation Centre, Eye Hospital, Wenzhou Medical University,
16 Wenzhou 325027, China

17 5 Peter Gorer Department of Immunobiology, School of Immunology & Microbial
18 Sciences, Faculty of Life Sciences & Medicine, King's College London, London SE1
19 7EH, UK

20 6 Department of Biosciences, Centre for Inflammation Research and Translational
21 Medicine, Brunel University, London UB8 3PH, UK

22 7 MFX (MicrofluidX) Ltd., Stevenage Bioscience Catalyst, Gunnels Wood Road,
23 Stevenage SG1 2FX, UK

¹ Lead Contact- Ciro Chiappini. Email- ciro.chiappini@kcl.ac.uk

24 **Summary**

25 Manufacturing cell and gene therapies (CGTs) at scale presents challenges in cost,
26 product consistency, and adaptability to personalised treatments. Traditional large-
27 volume bioreactors are designed to support cell growth through controlled nutrient
28 delivery and gas exchange, but are poorly suited to the decentralised, small-batch
29 production required for personalised therapies like Chimeric Antigen Receptor (CAR)
30 T-cells.

31 To address this, we have developed the KCL-Microbioreactor (K-MBR), a closed
32 microbioreactor platform based on microfluidic principles. Engineered in
33 polydimethylsiloxane (PDMS), the K-MBR combines spatial confinement, semi-
34 continuous perfusion, and integrated viral transduction in a compact footprint enabling
35 efficient gene delivery and robust expansion of therapeutic cells.

36 We demonstrate the platform's utility by generating functional CAR-Tregs targeting
37 HLA-A2, achieving a 92% increase in yield compared to conventional methods. The
38 K-MBR offers a streamlined, solution for CGT manufacturing, with potential to reduce
39 productions cost and enhance scalability across a broad range of cell therapies.

40 **Introduction**

41 The first engineered cell-based therapy was brought to market in 2017, with the FDA
42 approval of Kymriah- a chimeric antigen receptor (CAR)- T cell therapy for the
43 treatment of B-cell acute lymphoblastic leukaemia (B-ALL). Since then, there have
44 been additional CAR-T cell therapies approved by the FDA for the treatment of
45 haematological malignancies such as lymphoma, leukaemia and multiple myeloma.
46 By genetically engineering patient T-cells to express a CAR for a tumour-associated
47 antigen (TAA), CAR-T cells could recognise and induce apoptosis in tumour cells with
48 high specificity. CAR-T cell therapy has been demonstrated to have remarkable
49 efficacy as a cancer immunotherapy, with remission rates exceeding 90% in certain
50 patient groups¹.

51 While CAR-T cells are typically derived from a broad, undefined range of T-cell
52 subsets, often referred to collectively as pan T-cells, there is a growing field of
53 evidence supporting the use of CAR regulatory T-cells (Tregs) to modulate immune
54 responses². Derived from patient Tregs, which play a fundamental role in regulating

55 immune cell functions, CAR-Treg therapy can be used to alleviate immune-mediated
56 diseases by resolving aberrant immune responses. Alleles encoding the MHC class I
57 protein have been a key focal point of preclinical validation studies, with a range of
58 allograft models demonstrating long-term persistence and robust efficacy of HLA-A2-
59 specific CAR-Tregs (A2-CAR Tregs)³⁻⁵.

60 Ongoing first-in-human studies are now investigating the clinical applicability of A2-
61 CAR Tregs, in the context of solid organ transplantation and autoimmune diseases.
62 STEADFAST (TX200-TR101) is a phase I/II clinical trial, assessing the safety and
63 tolerability of A2-CAR Tregs in HLA-A2 mismatched renal transplantation⁶. A
64 preclinical assessment of TX200-TR101 demonstrated robust prevention of graft-
65 versus-host disease (GvHD) in a xenogeneic HLA-A2⁺ transplant model, highlighting
66 the capacity of antigen-specific CAR-Tregs to promote immune tolerance⁷. A similar
67 ongoing phase I/II clinical trial, LIBERATE (QEL-001), is investigating the safety and
68 clinical activity of A2-CAR-Tregs in A2-mismatched liver transplantation with early data
69 suggesting the therapy to be safe and well tolerated⁸. These findings support ongoing
70 efforts to translate CAR-Treg therapy into the clinic for targeted, antigen-driven
71 immunosuppression.

72 One of the key drawbacks that restricts the adoption of CAR-T cell therapies as a first-
73 or even second-line treatment is the high-price point that significantly restricts patient
74 accessibility. These therapies are typically autologous, requiring a patient-specific
75 manufacturing process involving skilled labour and expensive clinical-grade reagents
76 that are costly and difficult to scale. This involves isolating and activating T-cells, using
77 expensive viral vectors for stable gene expression, and expanding the cells ex vivo
78 over 6 to 14 days.

79 Closed-system cGMP-compliant platforms like the CliniMACS Prodigy enable
80 automated, end-to-end production of CAR-T cells⁹ and clinical-grade CAR-Tregs¹⁰.
81 These systems offer potential for decentralised, point-of-care manufacturing but face
82 challenges due to high upfront costs and lower process efficiencies compared to
83 modular platforms¹¹. These large-scale bioreactors use large fluid volumes to maintain
84 cell concentrations and nutrient supply, essential for producing CAR-based therapy
85 doses exceeding 10⁹ cells. However, this reduces culture efficiency, raising costs and
86 lowering yields. In these systems, viral transduction, with high-cost clinical-grade

87 lentiviruses, often results in low CAR-positivity rates (~30%), requiring high virus titres
88 and extended expansion times to achieve therapeutic doses¹².

89 Compared to such large-scale bioreactors, microbioreactors are emerging as
90 alternative platforms for cell therapy manufacturing, using significantly smaller working
91 volumes that offer increased process control and improved efficiencies. The
92 integration of microfluidic technology in biomanufacturing has the potential to
93 significantly streamline the production of CAR-T cell therapies by providing increased
94 precision and control over fluid dynamics and cell manipulation. By maintaining cells
95 at a high density, microfluidic systems can enhance the efficiency of key processes,
96 while allowing more accurate monitoring and regulation of culture conditions.
97 Microfluidic technology also offers the possibility of parallelising multiple steps within
98 the manufacturing process, allowing for a more continuous and automated production
99 line, thus minimising the need for extensive manual intervention.

100 A number of microfluidic approaches have been developed which support modalities
101 of a CAR-T cell manufacturing workflow including, but not limited to, cell isolation, high-
102 efficiency gene delivery and rapid expansion^{13,14}. A microfluidic device developed by
103 Moore et al., demonstrates the ability of using transmembrane flow to co-localise cells
104 and virus particles, driving high-efficiency viral transduction of primary, human T-
105 cells¹⁵. The use of inertial microfluidics can be used for the sorting of specific cell
106 populations, with Elsemary et al. demonstrating this approach for the purification of
107 viable CAR-T cells¹⁶. While such devices could be used in the context of CAR-T cell
108 manufacturing, the majority of these systems are confined to individual cell culture
109 operations.

110 Commercial microbioreactors such as the Quantum Cell Expansion System (Terumo
111 BCT), C.NEST (Cytena), and BioLector XT (Beckman Coulter) enable high-throughput
112 cell expansion with in-line monitoring. However, they lack the capabilities required to
113 support a broad spectrum of cell culture operations, limiting their suitability as end-to-
114 end platforms for CAR-T cell manufacturing^{17,18}. Only a small number of benchtop
115 microbioreactors have been commercialised with additional features tailored to CAR-
116 T workflows. The Mobius Breez (Merck) is a 2 mL single-use system designed for
117 high-throughput perfusion culture, integrating microfluidics and sensing controls.
118 Although early studies indicate its potential for CAR-T cell production¹⁹, evidence

119 supporting its compatibility with Tregs is limited. Moreover, the system is not currently
120 GMP-compliant, necessitating further validation and process transfer before use in
121 clinical or regulatory-grade settings.

122 While existing microbioreactors support many steps of the CAR-T cell manufacturing
123 workflow, they are not optimised for the specific needs of Treg culture and expansion,
124 with limited published evidence demonstrating their suitability for CAR-Treg
125 production. This highlights the need for a microbioreactor designed to address these
126 challenges and improve CAR-Treg manufacturing outcomes.

127 In order to overcome the aforementioned shortcomings of existing bioreactors, we
128 have developed a closed-system perfusion microbioreactor integrating the activation,
129 transduction and expansion steps required for the manufacturing of functional CAR-
130 Tregs from primary, human Tregs. By confining cells to a small fluidic volume while
131 optimising culture medium exchange parameters, this system could be used to
132 facilitate increases in both cell transduction efficiency and expansion capacity
133 compared to conventional systems. Using an optimised workflow, the K-MBR
134 supported a CAR-Treg manufacturing workflow with a 50% increase in expansion
135 capacity and a 92% increase in CAR-Treg yield, when compared to standard tissue
136 culture plasticware. Culture in the device had no observable impact on cell phenotype,
137 with generated A2-CAR-Tregs having the ability to potently suppress T-cell
138 proliferation in an antigen-dependent manner.

139 **Results**

140 **Device design and fabrication**

141 A systematic, iterative approach was used to design and fabricate a
142 polydimethylsiloxane (PDMS)-based microbioreactor (K-MBR) with a 1mL liquid
143 volume capable of supporting cell culture operations required in the CAR-Treg
144 manufacturing process. The K-MBR was composed of two PDMS components,
145 comprising a lower perfusion chamber and an upper bioprocessing chamber,
146 separated by a porous, polycarbonate membrane (**Figure 1**). The deposition of a thin
147 silica layer on each side of the polycarbonate membrane allowed the exposure of
148 hydroxyl groups (-OH) following oxygen plasma treatment, facilitating the formation of
149 strong covalent bonds with the PDMS components of the device. The use of

150 alternative chemical bonding methods, such as dipodal silanes or adhesives, resulted
151 in membrane fouling or loss of membrane integrity, especially when working with
152 fragile membranes. By using silica-sputtering, the membrane could be integrated in a
153 leak-free manner without any observable impact on membrane integrity (**Figure S1**).

154 The device was designed to support long-term cell culture directly on the membrane
155 surface, with a 5mm gaseous headspace in the bioprocessing chamber allowing for
156 aeration and efficient agitation. The small membrane pore size of 0.05 μ m ensured the
157 confinement of the virus particles in the bioprocessing chamber enhancing their
158 interactions with cells to support high-efficiency lentiviral transduction.

159 Each chamber was fitted with ports at either end of the device which could be closed
160 during cell culture to maintain sterility outside of a laminar flow hood. During cell
161 culture, spent culture medium in the perfusion chamber could be replaced at regular
162 intervals, or continuously, ensuring optimal nutrient replenishment and waste product
163 removal rates were met. The design features of the device, housing the perfusion
164 chamber directly below the porous membrane, resulted in a short diffusion pathway
165 between the two chambers, thus maximising the exchange of solutes.

166 **The K-MBR supports the culture of primary, human Tregs**

167 Freshly isolated human Tregs were introduced into the device and cultured for a 12-
168 day period with a manual 50% culture medium exchange every 3 days. Throughout
169 the culture, cells were sampled at regular intervals to establish both the cell counts
170 and viability (**Figure 2a,b**); device performance was compared to a 24-well plate with
171 the same cell seeding conditions and medium exchange regime. The K-MBR could
172 support the long-term culture of human Tregs, with no observed differences in viability
173 and mean fold expansion, compared to standard tissue culture plasticware. Flow
174 cytometric analysis was used to investigate cell phenotype, with a gating strategy
175 established to quantify proteins of interest (**Figure S2**). At day 12 post-seeding, there
176 was no observed effect on cell purity (CD4⁺CD25⁺ double positive cells) or phenotype
177 (**Figure 2c**).

178 Following a 12-day culture period, cells were harvested, re-suspended in fresh culture
179 medium and re-stimulated in their respective culture vessels. Cells were then cultured
180 for an additional 7 days, to investigate the potential of the device to support a second
181 round of simulation and sustained proliferation within a clinically relevant timeframe-

182 <3 weeks from initial isolation. The purpose of this assessment was therefore to
183 evaluate the maintenance of proliferative capacity after re-stimulation, rather than to
184 define the long-term growth kinetics. Robust expansion was demonstrated following
185 re-stimulation, showing that Tregs could be maintained in culture in the K-MBR for
186 multiple rounds of stimulation, without impacting the proliferative capacity of the cells
187 compared to standard tissue culture plasticware (**Figure 2d**).

188 **Rapid Treg expansion with optimised feeding regime**

189 Metabolite analysis revealed a significant build-up of lactate and ammonia (**Figure**
190 **S3**), alongside a depletion of glucose, with a 50% culture medium exchange every 3
191 days. Based on this information, an optimised regime was developed to maintain the
192 lactate concentration below 1.5g/L to prevent cell proliferation from being stunted
193 (**Figure 3a,b**). This threshold was not selected on the basis of lactate being intrinsically
194 inhibitory to Treg expansion, but rather as an operational limit to prevent nutrient
195 depletion, waste accumulation, and acidification in a system without active pH control.
196 While recent work has in fact demonstrated that lactic acid supplementation can
197 enhance Treg expansion, when pH is tightly regulated, in the K-MBR, rising lactate
198 levels were closely associated with glucose depletion and medium acidification (data
199 not shown). In the first three days of culture, 12.5% of the culture medium was
200 exchanged on a daily basis. From day 3 until day 9, 50% of the culture volume was
201 exchanged daily. In the final 3 days, 25% of the culture medium was exchanged each
202 day. This increasing frequency of culture medium exchange allowed efficient Treg
203 expansion in the K-MBR, achieving a 10-fold expansion over a 12-day period (**Figure**
204 **3c**). Treg expansion in the K-MBR was significantly higher than in a 24-well plate when
205 the same feeding regime was used, suggesting additional factors limiting Treg
206 expansion rate in the plate.

207 In a separate experiment, long-term Treg culture in the K-MBR was also compared to
208 the G-Rex 24-well plate, using an optimised cell expansion protocol. (ScaleReady).
209 By integrating a silicone membrane, G-Rex devices enable the rapid expansion of
210 suspension cells and are deemed as being the gold standard in the field for cell
211 expansion. Across a 12-day culture period, the K-MBR achieved robust Treg
212 expansion in-line with the G-Rex, with no impact on cell viability (**Figure 3d,e**).
213 Furthermore, the K-MBR operated with 5.1mL of culture medium, significantly less

214 than the 20mL required for the G-Rex expansion protocol (8mL starting volume with
215 two 6mL media exchanges).

216 **The K-MBR supports the production of CAR-Tregs**

217 In order to demonstrate the ability of the K-MBR to generate CAR-Tregs, the 12-day
218 workflow was adapted to include a 72-hour lentiviral transduction step (between day
219 3 and day 6 of culture), whereby lentivirus particles encoding a CAR targeting HLA-
220 A2 (A2-CAR) were introduced into the bioprocessing chamber of the device (Figure
221 4a). Following the 12-day process, Tregs expanded to a greater extent in the K-MBR
222 compared to a 24-well plate (**Figure 4b**) with no adverse impacts on cell phenotype
223 as they maintained a high purity (CD4⁺CD25⁺) with robust FoxP3, CTLA-4 and Ki-67
224 expression (**Figure 4c, f**).

225 With an MOI of 5, a transduction efficiency of 67% could be achieved in the K-MBR,
226 significantly higher than what was observed in the 24-well plate control (**Figure 4d**).
227 By confining cells and virus particles within a small fluid volume of 0.5mL in the
228 bioprocessing chamber, an increase in cell-virus interactions was likely responsible
229 for this improved transduction efficiency. While similarly low volumes can, in principle,
230 be used in standard 24-well plates, maintaining such volumes over multiple days is
231 constrained by evaporative loss, which leads to osmotic and pH shifts that can
232 adversely affect cell health. In our system, the closed-system nature of the device,
233 together with the regular media exchange regime, supported adequate nutrient and
234 gas exchange while keeping evaporation to a minimum, allowing the small working
235 volume to be maintained stably throughout culture. In a separate experiment,
236 introducing virus particles into the perfusion chamber of the device did not yield
237 transduction of cells in the bioprocessing chamber, demonstrating that the membrane
238 acted as a barrier preventing the movement of virus particles between chambers
239 (**Figure S4**). Using this manufacturing protocol, the K-MBR could generate CAR-Tregs
240 with a 92% increase in yield, compared to the 24-well plate (**Figure 4e**).

241 **A2-CAR-Tregs suppress T-cell proliferation *in vitro***

242 Following the 12-day workflow, Tregs were harvested and sorted based on their
243 expression of the reporter gene enhanced GFP (eGFP), allowing the purification of
244 A2-CAR-Tregs. Sorted A2-CAR-Tregs were co-cultured with HLA-A2⁺ or HLA-A2⁻ B-
245 LCLs for a 48-hour period, with flow cytometric analysis used to determine CAR-

246 mediated Treg activation via the expression of activation marker CD69. Significant
247 Treg CD69 upregulation was observed in the presence of HLA-A2 expressing B-LCLs
248 compared to Tregs cultured with HLA-A2 negative B-LCLs (**Figure 5a**). This
249 upregulation of CD69 was observed to the same extent in CAR-Tregs generated in
250 the K-MBR as those generated in the 24-well plate, suggesting that the CAR was
251 successfully being expressed following culture in both vessels.

252 In order to assess the ability of the CAR-Tregs to suppress the proliferation of effector
253 T-cells (Teffs), a suppression assay was performed. Prior to use in the assay, freshly
254 isolated Teffs were stimulated with TransAct™, in order to drive robust expansion
255 beyond that achievable with Dynabeads²⁰. Following isolation and *in vitro* expansion,
256 Teffs were frozen prior to being used for suppression assays. Cryopreserved donor-
257 matched Teffs were thawed and rested for 24 hours before being used. Tregs were
258 co-cultured with Teffs in the presence of either HLA-A2⁺ or HLA-A2⁻ B-LCLs. CAR-
259 Tregs were generated from HLA-A2⁻ Tregs to ensure that CAR-Tregs were not
260 stimulated by one another. As co-cultured Teffs did not express a synthetic receptor
261 targeting HLA-A2, the use of HLA-expressing B-LCLs ensured CAR-mediated
262 activation in the Tregs without Teff stimulation. After a 5-day co-culture, Teff
263 proliferation was assessed by the expression of the cell proliferation marker CellTrace
264 Violet. At day 5, it was observed that >95% Tregs exhibited eGFP expression,
265 demonstrating long-term, stable CAR expression. As expected, the A2-targeted CAR-
266 Tregs suppressed the Teff proliferation more potently in the presence of HLA-A2
267 antigen (**Figure 5b**). CAR-Tregs generated in the K-MBR were highly functional,
268 showing the ability to suppress the proliferation of Teffs to the same degree as CAR-
269 Tregs generated in a 24-well plate (**Figure 5c**), quantified by analysing the cell trace
270 violet (CTV) signal in proliferating Teffs (**Figure 5d**). These results demonstrate the
271 ability of the K-MBR to generate CAR-Tregs, with no impact on cell viability, phenotype
272 or function compared to standard tissue culture plasticware.

273 Discussion

274 The widespread adoption of CAR-based therapies is hampered by the complexity and
275 cost of the multi-step manufacturing process. The manipulation of a large fluid volume
276 in a typical bioreactor gives rise to batch heterogeneity and poor process efficiency. In
277 addition, such bioreactors typically have high upfront costs and require a need for

278 intensive labour, further driving up running costs. The K-MBR addresses these
279 shortcomings by demonstrating the potential of a device that supports the efficient
280 generation of functional CAR-Tregs using a significantly smaller working volume. It
281 was demonstrated that the K-MBR could be used to achieve the production of a
282 homogenous CAR-Treg population which suppressed the proliferation of Tregs in an
283 A2-dependent manner.

284 The 1mL volume, perfusion microbio reactor was developed to allow the high-density
285 culture and manipulation of primary, human Tregs. One of the key challenges faced in
286 developing a microbio reactor for the culture of suspension cells was integrating a
287 means of cell retention, to facilitate culture medium perfusion in the device. The use
288 of a porous membrane allowed Tregs to be maintained in culture while performing the
289 replacement of culture medium from the perfusion chamber below. By designing the
290 device with two separate fluidic chambers, culture medium could be replaced without
291 the risk of exerting shear stress on the cells. While culture medium was replenished
292 manually in a laminar flow hood, the integration of microfluidic ports gives rise to the
293 potential of culture medium perfusion being automated using a fluidic pump system.

294 Tregs could be stimulated and cultured in the device for a 12-day period, with no
295 impact on viability or phenotype compared to those cultured in standard tissue culture
296 plasticware. Using an optimised feeding regime, we were able to achieve a 150%
297 increase in Treg fold-expansion in the K-MBR compared to a standard feeding protocol
298 expanding cells from 1×10^6 to almost 1×10^7 in 12 days. Interestingly, we did not
299 observe an increase in Treg proliferation in plasticware with this optimised regime,
300 suggesting that there were additional factors limiting Treg growth. These data
301 demonstrate the ability of the K-MBR to support robust Treg expansion, supporting a
302 high cell density exceeding that achievable in standard tissue culture plasticware.

303 While the rate of nutrient replacement and waste removal was kept constant between
304 the K-MBR and 24-well plate, differences in materials and geometries between the
305 two culture vessels likely impacted the proliferative capacity of cells in culture. The use
306 of thin PDMS substrates ($< 2\text{mm}$) meant that gas exchange could occur between the
307 headspace and the surrounding environment in the incubator at a sufficient rate to
308 support rapid cell expansion. Unlike in a 24-well plate, whereby gas exchange only
309 occurs at the gas-liquid interface, within the K-MBR, gas exchange also occurs

310 through the sides of the device. The increased Treg growth rate observed in the K-
311 MBR may be the result of an increased oxygen transfer rate (OTR); further
312 experiments with the use of gas sensors could be implemented to characterise these
313 potential differences in gas exchange rates. The K-MBR supports the rapid expansion
314 of Tregs, in line with the capabilities of the G-Rex rapid expansion platform. The
315 degree of expansion achieved in the K-MBR was done so with 25% of the required
316 20mL in the G-Rex, demonstrating the potential of manufacturing steps being
317 performed in the microbioreactor in a low-cost manner.

318 Tregs could be transduced with high efficiency in the K-MBR, with an almost 2-fold
319 increase in CAR-Treg yield compared to standard tissue culture plasticware. The
320 increase in transduction efficiency observed in the K-MBR was likely due to an
321 increased degree of spatial confinement compared to the 24-well plate. While viruses
322 of the Retroviridae family have been demonstrated to travel in solution by Brownian
323 motion, estimates suggest that the relatively short half-life of these viruses limits their
324 displacement to around 500-600 μ m in a single half-life^{21,22}. As a result, a decrease in
325 liquid height is typically associated with increased cell-virus interactions, as suspended
326 virus particles are more likely to co-localise with sedimented cells.

327 With the 12-day CAR-Treg manufacturing workflow, a 6-fold expansion rate could be
328 achieved. While significantly higher than the expansion capacity achieved in standard
329 plasticware, a drop in expansion was observed compared to the 10-fold expansion
330 reached with wild type (WT) Tregs. The incorporation of viral transduction into the
331 workflow required a washing step to be performed at day 6, whereby cells were
332 removed from the device and washed to remove residual virus. This step, in
333 combination with the potential adverse effects of the lentiviral vector on cell health,
334 likely explains the drop in the expansion capacity of the engineered Tregs compared
335 to WT Tregs. Further device iterations could incorporate a means of flushing out virus
336 particles from the device while ensuring cell retention in the bioprocessing chamber,
337 therefore removing the need for a manual washing step.

338 CALR-Tregs generated in the K-MBR potently suppressed the proliferation of Tregs in
339 a 24-well plate, with no observable impact on cell function compared to those
340 generated in standard plasticware. While it has been demonstrated that CAR-T cell
341 phenotype/function can differ dramatically based on the device used to carry out the

342 manufacturing process¹¹, these data suggest that the effector functions of the CAR-
343 Tregs were not affected. The suppression observed was highly dependent on the
344 presence of HLA-A2 on the surface of the target cells, demonstrating the role of the
345 A2-CAR in driving CAR-Treg activation and function. As the most polymorphic MHC
346 allele group, with over 540 reported alleles, HLA-A2 mismatches are common in the
347 aetiology of GvHD and transplant rejection²³. A2-CAR-Tregs could be used to directly
348 target and suppress the proliferation of A2+ T-cells in the donor tissues or exert
349 bystander suppression in the local milieu surrounding the tissue, to prevent the onset
350 of GvHD and promote tissue tolerance.

351 Existing bioreactors used for autologous cell therapy manufacturing are limited in their
352 ability to support the generation of CAR-T cells in a highly efficient, closed-loop
353 manner. While such closed-loop bioreactors are commercially available, they are
354 plagued by batch heterogeneity, low process efficiency and still require a degree of
355 manual intervention. We demonstrate that the K-MBR perfusion microbioreactor can
356 generate functional CAR-Tregs targeting HLA-A2, in a highly efficient manner. The
357 perfusion microbioreactor supports high transduction efficiency and robust cell
358 expansion, comparable with the G-Rex platform. With a culture surface area of 1.5
359 cm², the K-MBR was able to support a cell density up to 6.5 x 10⁶ cells/cm², compared
360 to 5.0 x 10⁶ cells/cm² in the G-Rex platform, across a 12-day culture period. By
361 maintaining cells at a high density, our approach generates CAR-Tregs with a reduced
362 physical footprint compared to that of large-scale bioreactors. By further reducing
363 space and infrastructure requirements, it brings point-of-care cell therapy production
364 closer to feasibility, streamlining workflows and enabling a more accessible, patient-
365 specific approach. Moreover, our system has the potential to be fully automated,
366 aligning with the growing demand for more controlled and reproducible operations in
367 the CAR-Treg manufacturing process.

368 While further steps are necessary to demonstrate that such microbioreactors can be
369 scaled up further to reach the high final cell numbers achievable in large-scale
370 bioreactors, this research paves the way for the development of a closed-loop
371 microbioreactor suitable for clinical point-of-care CAR-Treg production.

372 **Resource availability**

373 **Lead contact**

374 Requests for further information and resources should be directed to and will be
375 fulfilled by the lead contact, [Ciro Chiappini \(ciro.chiappini@kcl.ac.uk\)](mailto:ciro.chiappini@kcl.ac.uk).

376 **Materials availability**

377 Materials from this study are available through [Ciro Chiappini](#) upon request.

378 **Data and code availability**

379 All data reported in this paper will be shared by [Ciro Chiappini](#) upon request; this paper
380 does not report original code. All datasets generated and analysed in this study,
381 including raw flow cytometry files and source data, are available from the lead contact
382 upon reasonable request.

383 **Limitations of Study**

384 One key limitation of this study is that all experiments were performed using cells from
385 healthy donors, and the performance of the K-MBR with patient-derived cells, including
386 those from immunocompromised or clinically relevant disease settings, remains to be
387 determined. While the platform was able to support high-density cell culture and
388 efficient CAR-Treg manufacturing at the laboratory scale, further work is required to
389 demonstrate robust scale-out, integration of automation, and compatibility with fully
390 cGMP-compliant workflows. In addition, although comparable outcomes were
391 observed across devices, a more comprehensive assessment of inter-device
392 variability and long-term process reproducibility is necessary to support clinical
393 manufacturing. Functional characterisation was limited to *in vitro* assays, and *in vivo*
394 persistence, stability and safety of CAR-Tregs generated in the K-MBR were not
395 evaluated.

396 **Acknowledgments**

397 **Funding statement**

398 C.C. acknowledges funding from the European Union under the ERC Starting Grant
399 ENBION 759577 and the medical research council under the Confidence in Concept
400 award (MC_PC_18052); Medical Research Council (MRC); MFX (MicrofluidX) Ltd.
401 acknowledges funding from the MRC DTP iCASE Studentship Scheme.

402 **Author Contributions**

403 **W.E.**- contributed methodology, investigation, formal analysis, project administration,
404 writing of original draft; **N.S.**- contributed methodology, investigation and formal
405 analysis; **Y.W.**- contributed methodology, investigation and formal analysis; **Y.L.**-
406 contributed methodology, investigation and formal analysis **C.W.**- contributed
407 methodology and investigation; **D.M.**- contributed methodology and investigation;
408 **C.S.**- contributed methodology and investigation; **M.R.**- contributed methodology and
409 investigation; **C.M.C** and **A.E.** - contributed conceptualisation and consultation as well
410 as provided additional funding and in-kind contributions, e.g. use of company facilities
411 and resources; **G.L.**- contributed supervision, methodology, formal analysis and
412 project administration; **C.C.**- conceptualisation, funding acquisition, methodology,
413 project administration, supervision, visualisation and writing of original draft.

414 **Declaration of Interests**

415 G.L. is a Founder and consultant of Quell Therapeutics. C.M.C. and A.E. are
416 founders and shareholders of MFX Ltd. The other authors declare no interests.

417 **Figure Titles and Legends**

418 **Figure 1- Microbioreactor Fabrication.** (a) Orthogonal view of microbioreactor,
419 showing multiple components of the device. (b) Side-view of microbioreactor
420 demonstrating two sets of ports used for A) perfusing the system with fresh culture
421 medium or B) seeding the device with cells. (c) Microbioreactor components. (d)
422 Assembled microbioreactors, filled with culture medium.

423 **Figure 2- K-MBR supports Treg Expansion.** Compared to a 24-well plate, the K-
424 MBR device had no adverse impact on cell (a) proliferation, (b) viability or (c)
425 phenotype. (d) over a 12-day period (n=3 devices). Cells could be re-stimulated and
426 maintained in culture for an additional 7 days with no impact on cell proliferation.
427 Statistical significance was determined by one-way ANOVA for timepoint experiments;
428 for day 12 analysis; for flow cytometric analysis t-tests with Šídák correction for
429 multiple comparisons; error bars representing mean \pm SEM.

430 **Figure 3- Optimised Treg Expansion in K-MBR** a) Feeding regime optimisation for
431 a 12-day Treg expansion; VVD = vessel volumes per day. b) An increased culture
432 medium replacement frequency (regime 2) resulted in a reduction in lactate build-up
433 during Treg culture, in a 24-well plate. c) Treg expansion in the K-MBR compared to

434 a 24-well plate; data from independent experiments with cells from 3 healthy donors
435 ($n = 9$ devices). **d)** Treg expansion and **e)** day 12 viability in the K-MBR compared to
436 the G-Rex 24-well plate ($n = 2$ devices). Statistical significance was determined by
437 one-way ANOVA for timepoint comparisons and unpaired t-test for day 12 viability;
438 error bars representing mean \pm SEM. **: $P \leq 0.01$.

439 **Figure 4- CAR-Tregs generation with K-MBR.** **a)** CAR-Treg 12-day manufacturing
440 workflow, with manual steps and media exchanges shown; LV = lentivirus. **b)** Treg
441 expansion. Day 12 assessment of **c)** cell phenotype, **d)** transduction efficiency and **e)**
442 total CAR-Treg yield. Two independent experiments with cells from 2 healthy donors
443 ($n = 6$ devices) **f)** representative flow plots for Treg phenotyping. Statistical significance
444 was determined by one-way ANOVA for timepoint experiments; for day 12 analysis;
445 for flow cytometric analysis t-tests with Šídák correction for multiple comparisons; error
446 bars representing mean \pm SEM. *: $P \leq 0.05$, **: $P \leq 0.01$, ***: $P \leq 0.001$.

447 **Figure 5- Suppression Ability of K-MBR generated Tregs is preserved.** **a)** Surface
448 expression of activation marker CD69 assessing the ability of CAR-Tregs to respond
449 to target antigen ($n = 2$ devices). Suppression assay with cells from 2 healthy donors
450 ($n = 6$ devices) in independent experiments to assess. **b)** CAR-Tregs suppression T-
451 cell proliferation in response to target antigen in a 24-well plate. **c)** Impact of K-MBR
452 culture on CAR-Treg suppressive capacity in the presence of either HLA-A2⁺ B-LCLs
453 or HLA-A2⁻ B-LCLs. **d)** representative flow cytometry plots of proliferating Tregs
454 following 5-day suppression assay. Statistical significance was determined by mixed-
455 model two-way ANOVA for suppression assays; for CD69 expression analysis t-tests
456 with Šídák correction for multiple comparisons; error bars representing mean \pm SEM.
457 *: $P \leq 0.05$, ****: $P \leq 0.0001$.

458 **Figure 6- Schematic of HLA-A2 CAR construct.** CAR- chimeric antigen receptor;
459 eGFP- enhanced green fluorescent protein. Adapted from Boardman et al. (2017)³.

460 **Main Tables and Legends**

Cell type	Culture medium	Supplementation
Tregs	X-VIVO 15	IL-2 (1,000 IU/mL) Rapamycin (100nM)
T-cells	X-VIVO 15	IL-2 (100 IU/mL)
B-LCLs	RPMI-1640	Heat-inactivated FBS (10% v/v) Penicillin (100 IU/mL) Streptomycin (100 ug/mL) GlutaMAX (1mM)

461 **Table 1- Culture media and supplementation used for different cultured cell types.**

Marker	Fluorophore	Clone	Supplier
CD4	BV605	SK3	BioLegend
CD25	PE	BC96	BioLegend
CD69	PE-Cy7	FN50	BioLegend
CD127	BV785	A019D5	BioLegend
HLA-A2	PE	BB7.2	Bio-Techne
FoxP3	Alexa Fluor 647	206D	BioLegend
Ki-67	BV510	11F6	BioLegend
CTLA-4	PerCP-Cy5.5	BNI3	BioLegend

462 **Table 2- Antibody panel for T-cell/Treg characterisation.**

463 STAR Methods

464 Experimental model and study participant details

465 Epstein-Barr Virus (EBV) transformed cell lines

466 Cryopreserved B-lymphoblastic cell lines (B-LCLs) were thawed and re-suspended at
 467 0.2×10^6 cells/mL in supplemented RPMI-1640 with the addition of 1mM glutaMAX
 468 (Gibco), 10% heat-inactivated foetal bovine serum (FBS), 100 IU/mL penicillin and 100
 469 μ g/mL streptomycin (ThermoFisher, UK). Cells were maintained in culture (5% CO₂,
 470 37°C) at an appropriate density and expanded to reach suitable cell numbers prior to

471 use. The Epstein-Barr Virus (EBV) transformed cell lines SPO B-LCLs (HLA-A2⁺) and
472 BM21 B-LCLs (HLA-A2⁻) (Merck) are part of the Human Leukocyte Antigen (HLA)
473 Typed Collection maintained by the European Collection of Cell Cultures (ECACC)
474 and were obtained from Boardman et al.³. These cells were originally derived from a
475 peripheral B cell line established from a male donor. Before use, cryopreserved cell
476 lines were thawed and re-suspended in pre-warmed culture medium before being
477 rested overnight. The next day, cells were collected and re-suspended in fresh culture
478 medium to remove residual DMSO, prior to use for cell culture experiments. Cell line
479 authentication testing was not performed. All cell lines tested negative for mycoplasma
480 contamination prior to experimental use.

481 *Primary T-cells*

482 For cell culture experiments, Tregs were re-suspended at 1×10^6 cells/mL in X-VIVO
483 15 culture media (Lonza) supplemented with 1,000 IU/mL IL-2 and 100nM rapamycin.
484 Human T-Activator CD3/CD28 Dynabeads™ (Thermo Fisher Scientific) were added
485 at a 1:1 cell to bead ratio and cells were maintained in culture for up to 12 days.
486 Dynabeads were selected as a source of CD3/CD28 antigens for Tregs, with data
487 demonstrating their ability to drive robust expansion compared to other stimulation
488 methods²⁵. At day 12, Dynabeads™ were magnetically removed and cells were
489 washed and re-suspended in culture medium at 1×10^6 cells/mL with the addition of
490 fresh Dynabeads™ when re-stimulation was required. For culture in the G-Rex 24-
491 well plate, an optimised cell expansion protocol was used (ScaleReady), whereby $1 \times$
492 10^6 Tregs were seeded in 8mL, with the replacement of 6mL culture medium at day 4
493 and day 8.

494 Teffs were re-suspended at 1×10^6 cells/mL unless otherwise stated, in X-VIVO 15
495 culture medium supplemented with 100 IU/mL IL-2. T cell TransAct™ (Miltenyi Biotec)
496 was added according to the manufacturer's protocol (1:100 titre) and cells were
497 maintained in culture for up to 12 days. Re-stimulation was performed by washing cells
498 and re-suspending in culture medium with fresh T cell TransAct™. The various
499 supplemented culture media used for different cell types is summarised (Error!
500 Reference source not found.).

501 **Method details**

502 *Replica moulding and K-MBR assembly*

503 A CO₂ laser-ablated (Trotec) polymethylmethacrylate (PMMA) negative mould was
504 designed and fabricated for each of the two PDMS components of the K-MBR
505 microbioreactor. Following replica moulding, 2mm port holes were punched in the top
506 PDMS substrate, which contained the bioprocessing chamber. These ports made it
507 possible to access both the bioprocessing and perfusion chambers of the device,
508 allowing fluid manipulation.

509 *Membrane silica deposition*

510 To facilitate the bonding between the polycarbonate membrane and PDMS substrates,
511 a silica (SiO₂) intermediate layer was deposited on both sides of the membranes using
512 a previously described approach²⁴. A magnetron SF sputterer (Korvus Technology)
513 was used (100 W RF power, 35 minutes on each side, with an argon flow rate of 32
514 sccm and oxygen flow rate of 8 sccm) to deposit SiO₂ on both sides of the
515 polycarbonate membrane, resulting in a SiO₂ intermediate layer with a thickness of
516 around 100 nm on each side of the membrane. The sputtered membrane was laser
517 cut to size before being exposed to oxygen plasma on both sides (100W, 50sccm, 1
518 minute) along with the two PDMS components. Device components were brought into
519 conformal contact with one other and the assembled device was incubated at 80°C for
520 30 minutes to ensure strong bonding between the device components.

521 *K-MBR device preparation and use*

522 Assembled devices were fitted with polyetheretherketone (PEEK) tubing (Cole-
523 Parmer), secured using silicon adhesive, and attached to silicon tubing (VWR)
524 allowing fluid manipulation in a leak-free manner. For cell culture experiments, ports
525 were closed using luer plugs (microfluidic Chip Shop) to maintain sterility in the
526 devices. Prior to use, the K-MBR was either flushed with 70% ethanol or steam
527 autoclaved at 121°C for 15 minutes, before being rinsed thoroughly with sterile PBS
528 and equilibrated with culture medium for a minimum of 2 hours.

529 *Cell handling*

530 All aseptic cell culture was performed in class II biological safety cabinets, with
531 cultured cells being kept in all cases in incubators at 37°C, supplied with 5% CO₂.
532 Cells were typically washed and pelleted using 300g centrifugation at 4°C, unless
533 stated otherwise. Cell counts were obtained either manually using trypan blue dye
534 (Sigma-Aldrich) and a haemocytometer, or with a NucleoCounter NC-202

535 (ChemoMetec). For cell counts and viability measurements prior to experimental end-
536 points, cell suspensions were mixed thoroughly by pipetting, and a 20 μ L aliquot was
537 taken for analysis

538 *Primary T-cell isolation*

539 Cells were isolated from leukocyte cones obtained from the NHSBT (National Health
540 Service Blood and Transplantation, Tooting, London, UK), obtained from anonymised
541 healthy volunteers with informed consent. Peripheral blood from leukocyte cones was
542 diluted 1:1 in PBS and incubated at room temperature for 20 minutes with RosetteSep
543 Human CD4⁺ T Cell Enrichment Cocktail (StemCell Technologies). The reagent
544 contains antibody complexes that crosslink CD4⁻ cells with glycophorin A on
545 erythrocytes, allowing the isolation of CD4⁺ cells by negative selection. Following
546 incubation, blood samples were diluted further with PBS and layered onto Lymphoprep
547 density gradient medium (StemCell Technologies). Samples were then centrifuged at
548 600g for 20 minutes with low acceleration and deceleration, facilitating the separation
549 of lymphocytes by density gradient centrifugation. CD4⁺ peripheral blood lymphocyte
550 cells (PBMCs) were isolated from the interphase layer, washed twice with PBS and
551 re-suspended in magnetic-activated cell sorting (MACS) buffer- PBS supplemented
552 with 0.5% bovine serum albumin (BSA) and 5mM Ethylenediaminetetraacetic acid
553 (EDTA), at 1×10^7 cells/mL.

554 The cell suspension was mixed with CD25 Microbeads II (Miltenyi Biotec) and
555 incubated at 4°C for 15 minutes. Cells were washed and re-suspended at 2×10^8
556 cells/mL in MACS buffer before being passed through a MACS LS column placed on
557 a magnetic stand (Miltenyi Biotec). The column was rinsed three times with MACS
558 buffer, washing out CD25⁻ cells while capturing bead-bound CD25⁺ cells in the column.
559 The column was then removed from the magnetic stand and a plunger was used to
560 force 5mL MACS buffer through the column, eluting the CD25⁺ fraction. This
561 CD4⁺CD25⁺ population has been demonstrated to exhibit high expression of the
562 canonical Treg marker FoxP3. CD4⁺CD25⁺ Tregs were used fresh for all cell culture
563 experiments while CD4⁺CD25⁻ T effs were either used fresh for cell culture experiments
564 or cryopreserved for use in suppression assays. For cryopreservation, cells were re-
565 suspended between 1×10^7 and 5×10^7 cells/mL in freezing medium composed of
566 90% heat-inactivated fetal bovine serum (FBS) (Gibco) and 10% dimethyl sulfoxide

567 (DMSO) (Sigma-Aldrich). Cells were stored at -80°C overnight before being
568 transferred to liquid nitrogen for long-term storage.

569 *Flow Cytometry*

570 For phenotypic analysis using flow cytometry, between 0.1 - 0.5 x 10⁶ cells were re-
571 suspended in 100µL PBS per sample with the addition of antibodies for antigens of
572 interest, according to the manufacturers' protocols. For viability testing, LIVE/DEAD™
573 Fixable Near-IR Dead Cell Stain (Invitrogen) was included in the panel at a dilution of
574 1:1,000. Samples were incubated at 4°C for 20 minutes before being washed with 1mL
575 PBS. For intracellular staining, cells were fixed and permeabilised using Foxp3/
576 Transcription Factor Fixation/Permeabilization kit (Invitrogen) for 30 minutes before
577 being washed and re-suspended in 100µL permeabilisation buffer containing
578 intracellular antibodies. Samples were incubated at 4°C for 30 minutes before being
579 washed with PBS and re-suspended in 300µL PBS before acquisition on the BD
580 LSRFortessa analyser (BD Biosciences). A panel of anti-human antibodies was used
581 for the characterisation of human T-cells and Tregs, to assess cell purity and function
582 (**Table 2**).

583 Anti-FoxP3, Ki-67 and CTLA-4 antibodies were used to quantify the intracellular
584 expression of these proteins; all others listed were used to quantify surface marker
585 expression.

586 *Fluorescence-activated cell sorting (FACS)*

587 Following the 12-day full CAR-Treg manufacturing process, harvested Tregs had their
588 anti-CD3/CD28 Dynabeads™ removed and were re-suspended at 1 x 10⁷ cells/mL in
589 PBS and sorted into sterile tubes containing X-VIVO 15 culture medium based on
590 eGFP expression using a BD FACS Aria II (BD Biosciences). Sorted GFP⁺ CAR-Tregs
591 were re-suspended in X-VIVO 15 at the required concentration and used for
592 downstream operations.

593 *Purity testing and HLA typing*

594 Following cell isolation and prior to cell culture experiments, cells were stained and
595 flow cytometric analysis was performed to assess cell viability and purity. Following
596 the selection of single, live lymphocytes, using the aforementioned gating strategy,

597 Treg purity was assessed by quantifying the surface expression of CD4 alongside the
598 expression of additional markers- CD25, CD127 and FoxP3.

599 For cell culture experiments that required HLA haplotyping, a 10 μ L blood sample was
600 taken during the cell isolation process and incubated with 200 μ L Ack Lysing buffer
601 (Gibco) for 5 minutes to lyse red blood cells (RBCs). Samples were washed with PBS
602 and labelled with anti-human HLA-A2 (Bio-Techne) for flow cytometric analysis.

603 *Antigen specific activation*

604 Both HLA-A2⁺ and HLA-A2⁻ B-LCLs were firstly incubated at 1 x 10⁷ cells/mL in
605 50 μ g/ μ L mitomycin C (Sigma-Aldrich) solution for 50 minutes at 37°C before being
606 washed with PBS and re-suspended in X-VIVO 15. By inhibiting DNA synthesis,
607 mitomycin C was used to inhibit B-LCL cell proliferation without impacting their ability
608 to stimulate Tregs. To determine CAR-specific Treg activation, sorted A2 CAR-Tregs
609 were co-cultured with either the HLA-A2⁺ or HLA-A2⁻ B-LCLs at a ratio of 2:1 Tregs to
610 B-LCLs, in a 96-well round bottomed plate.

611 Following 48 hours of culture, cells were harvested and washed with PBS before being
612 stained for LIVE/DEAD, CD4 and CD69, as previously described. Cells were washed
613 and re-suspended in PBS before acquisition, to assess the degree of antigen specific
614 Treg activation. CAR-Tregs were identified as live CD4⁺ cells expressing the lentiviral-
615 CAR (LV-CAR) eGFP reporter gene, with the quantification of CD69 surface
616 expression demonstrating the degree of Treg activation. Tregs were also cultured in
617 the absence of B-LCLs, to identify the baseline CD69 expression of unstimulated
618 Tregs.

619 *Treg suppression assay*

620 Sorted CAR-Tregs were re-suspended at 1 x 10⁶ cells/mL in X-VIVO 15 and serial
621 diluted in wells of a 96-well round bottomed plate. Autologous Teffs were incubated at
622 1 x 10⁷ cells/mL in 5 μ M cell trace violet (CTV) solution at 37°C for 20 minutes before
623 being topped up with culture medium and incubated for a further 5 minutes at 37°C.
624 CTV staining can be used to monitor cell proliferation, with each subsequent
625 generation of proliferating cells expressing a lower CTV signal as a result of dye
626 dilution²⁶. Following staining, Teffs were re-suspended in X-VIVO 15 at 2 x 10⁶
627 cells/mL and added to the plate, with 50 μ L CTV-labelled Teffs per well. By serial

628 diluting the CAR-Tregs, a range of Treg:Teff ratios could be achieved in the plate,
629 spanning from 1:1 to 1:64.

630 Mitomycin C treated B-LCLs, either HLA-A2⁺ or HLA-A2⁻ were re-suspended at 1×10^6
631 cells/mL and 50 μ L cell suspension was added per well, to achieve a final volume in
632 each well of 200 μ L. Cells were co-cultured for a 5-day period before being analysed
633 with flow cytometry to assess the degree of Teff proliferation in each sample. The
634 degree by which CAR-Tregs suppressed Teff proliferation was determined by taking
635 the inverse of Teff proliferation (CTV^{lo}) and normalising it to Teff proliferation when
636 stimulated with anti-CD3/CD28 Dynabeads™ at a 40:1 cell to bead ratio.

637 A gating strategy was used to firstly identify eGFP⁻ Teffs before gating on CTV^{lo} cells
638 to quantify the degree of Teff proliferation and hence the suppressive capacity of the
639 co-cultured CAR-Tregs.

640 *Metabolite analysis*

641 For metabolite analysis, a minimum volume of 150 μ L supernatant was collected from
642 cell culture vessels and analysed using the BioProfile FLEX2 (Nova Biomedical) with
643 chemistry and osmometry modules. For supernatant sampling in the K-MBR, spent
644 culture medium was collected from the perfusion chamber. When working with sample
645 sizes <150 μ L, samples were diluted with Milli-Q water, with calculations performed
646 accordingly to account for the dilution factor.

647 *Chimeric antigen receptor (CAR) construct*

648 A previously described lentiviral HLA-A2 -CAR, with a CD28 hinge domain, CD28-
649 CD3 ζ signalling domain and an enhanced green fluorescent protein (eGFP) reporter
650 gene under an SFFV promoter³ (**Figure 6**) was used for the transduction of primary,
651 human Tregs to generate CAR-Tregs targeting HLA-A2. As previously described,
652 HEK293T cells were co-transfected with the transfer plasmid, p Δ 8.91 and pCMV-VSV-
653 G plasmids at a mass ratio of 4:3:1 using polyethylenimine (3:1 PEI:DNA wt/wt; Sigma-
654 Aldrich, Gillingham, Dorset, UK). Viral supernatant was collected 48–56 hours post-
655 transfection, and lentiviral particles were concentrated using PEG-it™ (System
656 Biosciences, Bar Hill, Cambridgeshire, UK).

657 *Lentiviral transduction*

658 For the transduction of primary human T-cells and Tregs, cells were typically
659 stimulated for 72 hours prior to being washed and re-suspended in fresh culture
660 medium. Viral particles were thawed and added directly to the cell suspension at the
661 required concentration to achieve the desired MOI. When performing the full CAR-
662 Treg manufacturing process in the K-MBR microbioreactor and 24-well plate control,
663 cells were counted at day 3 post-seeding and the viral vector was added directly to the
664 culture vessel at the required concentration, following a 50% culture medium
665 exchange.

666 Following the required transduction period, typically 72 hours unless stated otherwise,
667 cells were harvested and washed. For the full CAR-Treg manufacturing process in the
668 K-MBR microbioreactor and 24-well plate, cells were re-suspended in fresh culture
669 medium and returned to the corresponding culture vessel. One of two methods was
670 used for determining transduction efficiency, depending on the LV-CAR used. For cells
671 transduced with the HLA-A2 LV-CAR, transduction efficiency was determined by
672 quantifying eGFP reporter gene expression using flow cytometry

673 *Virus precipitation*

674 PEG-it virus precipitation solution (System Biosciences) was used for the precipitation
675 of virus particles from cell culture supernatants. Supernatants were re-suspended in
676 PEG-it solution and refrigerated at 4°C overnight. 12 hours after re-suspension, the
677 supernatant-containing solution was centrifuged to pellet the virus particles (1,500 x
678 g, 30 minutes, 4°C) and all residual fluid was carefully aspirated. Lentivirus particles
679 were then re-suspended in X-VIVO 15 culture media at the desired concentration.

680 *Bright-field and immunofluorescence*

681 Both bright-field and immunofluorescence imaging were performed on a Leica DMI8
682 inverted microscope (Leica Microsystems). The tile scanning feature was used in the
683 Leica LAS X software, for bioprocessing chamber live imaging.

684 *Scanning electron microscopy*

685 Scanning electron microscopy (SEM) images were captured using a Carl Zeiss
686 XB1540 Crossbeam SEM/FIB equipped with an InLens detector, operated at 3 kV.
687 Prior to imaging, the samples were sputter-coated with gold using a sputter coater
688 (Edwards Ltd.).

689 **Quantification and statistical analysis**

690 *Flow cytometric analysis*

691 A typical manual gating strategy was used for flow cytometric analysis with FlowJo
692 software, with sequential gating performed on lymphocytes, single cells and live cells
693 prior to the quantification of any other markers. This gating strategy was used in all
694 flow cytometric analyses, unless otherwise stated, prior to the analysis of additional
695 marker expression levels.

696 *Statistical analysis*

697 All data plotted in graphs were presented as mean values with standard error of the
698 mean. Statistical tests were performed using Graphpad Prism, as described in figure
699 legends. For timepoint experiments, assessing cell growth in the K-MBR and standard
700 tissue culture plasticware, a one-way ANOVA was used. For the analysis of flow
701 cytometric data at a single timepoint, for example, day 12 post-seeding, t-tests with
702 Šídák correction for multiple comparisons was performed. For the comparison of Treg
703 suppression following culture in the K-MBR and standard tissue culture plasticware,
704 differences in curves were assessed with a mixed-model two-way ANOVA. Unless
705 otherwise stated, plotted error bars for pooled data represent mean \pm SEM. For all
706 statistical tests performed, statistical significance was illustrated according to the
707 following p-value cutoffs:

708 ns: $P > 0.05$; *: $P \leq 0.05$; **: $P \leq 0.01$; ***: $P \leq 0.001$; ****: $P \leq 0.0001$

709 **Supplemental Information**

710 **Supplementary Figure 1-** *Images of membranes before and after silica deposition.*
711 *The membrane was sputtered with ~100nm SiO₂ with a) photo and b) SEM images of*
712 *membranes. In both, left- untreated membrane, right- silica-sputtered membrane.*

713 **Supplementary Figure 2-** *Typical flow cytometry gating strategy used. A) A gating*
714 *strategy was used to gate on live, single, lymphocytes prior to any additional gating.*
715 *B) An example of the gating strategy used to identify the proportion of GFP⁺ Tregs*
716 *expressing the activation marker CD69.*

717 **Supplementary Figure 3-** *Metabolite analysis on supernatant from 12-day Treg*
718 *culture, sampled from the perfusion chamber of the K-MBR. Concentrations of*

719 *glucose, glutamine, lactate and ammonia over time were investigated. Supernatant*
720 *samples were collected at regular timepoints from the cells of two healthy donors, in*
721 *independent experiments.*

722 **Supplementary Figure 4-** *The ability of the membrane to support high-efficiency viral*
723 *transduction in the K-MBR. K-MBR was seeded with stimulated Tregs and spiked with*
724 *virus particles in either the bioprocessing (BP) chamber or perfusion (P) chamber.*
725 *Transduction efficiency was assessed after 72 hour and compared to an un-*
726 *transduced control. BP chamber = bioprocessing chamber; P = perfusion chamber.*
727 *Statistical significance was determined with a One-way ANOVA. ****: $P \leq 0.001$.*

728 **References**

- 729 1. Gardner RA, Finney O, Annesley C, Brakke H, Summers C, Leger K, et al.
730 Intent-to-treat leukemia remission by CD19 CAR T cells of defined formulation
731 and dose in children and young adults. *Blood* [Internet]. 2017 Jun 22 [cited
732 2019 Apr 16];129(25):3322–31. Available from:
733 <http://www.ncbi.nlm.nih.gov/pubmed/28408462>
- 734 2. Mohseni YR, Tung SL, Dudreuilh C, Lechler RI, Fruhwirth GO, Lombardi G.
735 The Future of Regulatory T Cell Therapy: Promises and Challenges of
736 Implementing CAR Technology [Internet]. Vol. 11, *Frontiers in Immunology*.
737 Frontiers Media S.A.; 2020 [cited 2021 Jun 15]. p. 1608. Available from:
738 www.frontiersin.org
- 739 3. Boardman DA, Philippeos C, Fruhwirth GO, Ibrahim MAA, Hannen RF, Cooper
740 D, et al. Expression of a Chimeric Antigen Receptor Specific for Donor HLA
741 Class I Enhances the Potency of Human Regulatory T Cells in Preventing
742 Human Skin Transplant Rejection. *Am J Transplant* [Internet]. 2017 Apr 1
743 [cited 2024 May 8];17(4):931–43. Available from:
744 <https://pubmed.ncbi.nlm.nih.gov/28027623/>
- 745 4. MacDonald KG, Hoeppli RE, Huang Q, Gillies J, Luciani DS, Orban PC, et al.
746 Alloantigen-specific regulatory T cells generated with a chimeric antigen
747 receptor. *J Clin Invest* [Internet]. 2016 Apr 1 [cited 2024 May 8];126(4):1413–
748 24. Available from: <https://pubmed.ncbi.nlm.nih.gov/26999600/>
- 749 5. Noyan F, Zimmermann K, Hardtke-Wolenski M, Knoefel A, Schulde E, Geffers

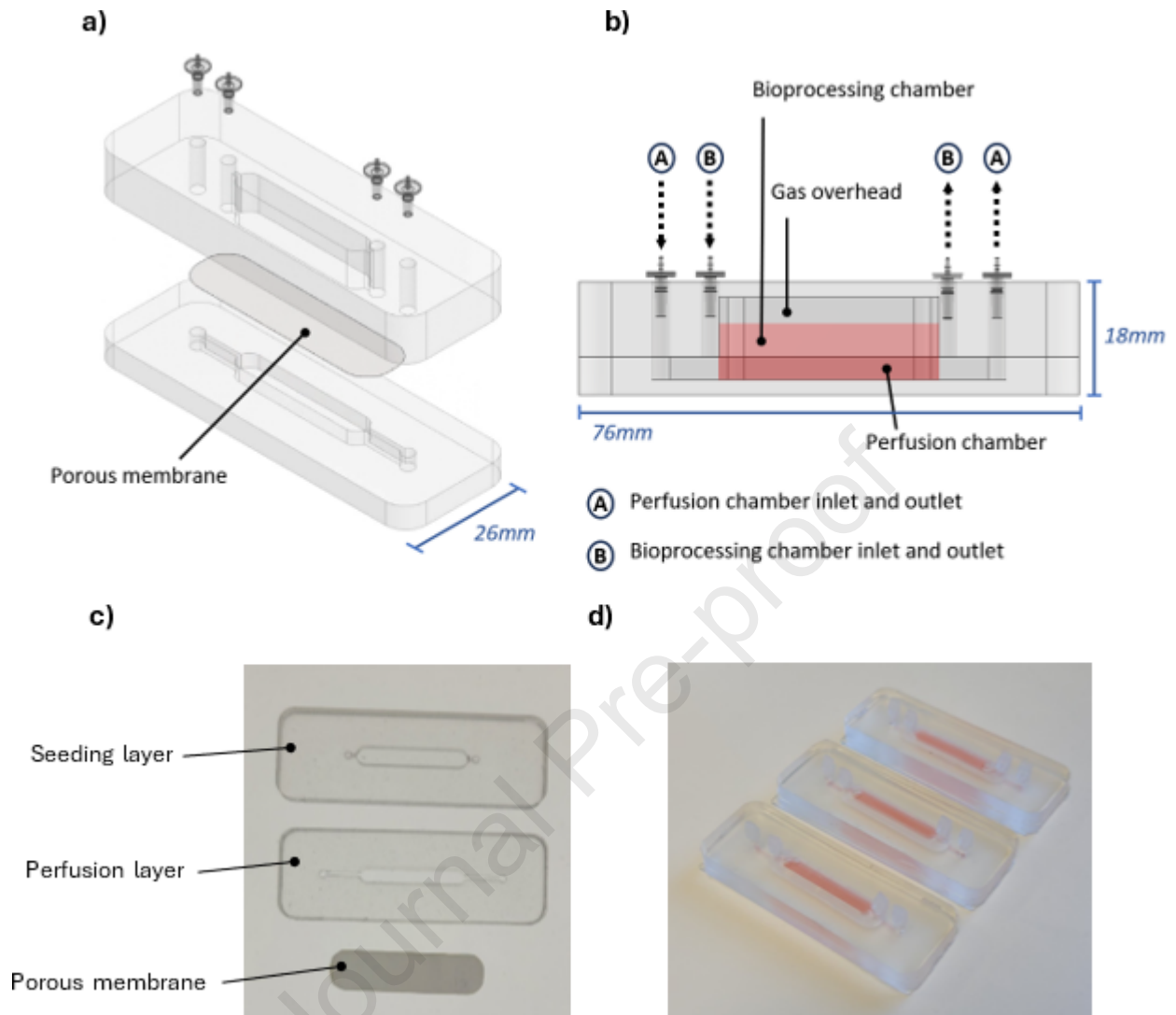
- 750 R, et al. Prevention of Allograft Rejection by Use of Regulatory T Cells With an
751 MHC-Specific Chimeric Antigen Receptor. *Am J Transplant* [Internet]. 2017
752 Apr 1 [cited 2025 Jul 3];17(4):917–30. Available from:
753 <https://www.amjtransplant.org/action/showFullText?pii=S1600613522249338>
- 754 6. Schreeb K, Culme-Seymour E, Ridha E, Dumont C, Atkinson G, Hsu B, et al.
755 Study Design: Human Leukocyte Antigen Class I Molecule A*02-Chimeric
756 Antigen Receptor Regulatory T Cells in Renal Transplantation. *Kidney Int*
757 *Reports*. 2022 Jun 1;7(6):1258–67.
- 758 7. Proics E, David M, Mojibian M, Speck M, Lounnas-Mourey N, Govehovitch A,
759 et al. Preclinical assessment of antigen-specific chimeric antigen receptor
760 regulatory T cells for use in solid organ transplantation. *Gene Ther*. 2023 Apr
761 1;30(3–4):309–22.
- 762 8. Bluestone JA, McKenzie BS, Beilke J, Ramsdell F. Opportunities for Treg cell
763 therapy for the treatment of human disease. *Front Immunol* [Internet]. 2023
764 [cited 2025 Jul 2];14:1166135. Available from:
765 <https://pmc.ncbi.nlm.nih.gov/articles/PMC10154599/>
- 766 9. Palani HK, Arunachalam AK, Yasar M, Venkatraman A, Kulkarni U, Lionel SA,
767 et al. Decentralized manufacturing of anti CD19 CAR-T cells using CliniMACS
768 Prodigy®: real-world experience and cost analysis in India. *Bone Marrow*
769 *Transplant* [Internet]. 2023 Feb 1 [cited 2025 Feb 12];58(2):160–7. Available
770 from: <https://pubmed.ncbi.nlm.nih.gov/36347999/>
- 771 10. Marín Morales JM, Münch N, Peter K, Freund D, Oelschlägel U, Hölig K, et al.
772 Automated Clinical Grade Expansion of Regulatory T Cells in a Fully Closed
773 System. *Front Immunol* [Internet]. 2019 [cited 2025 Feb 12];10(FEB). Available
774 from: <https://pubmed.ncbi.nlm.nih.gov/30778344/>
- 775 11. Song HW, Somerville RP, Stroncek DF, Highfill SL. Scaling up and scaling out:
776 Advances and challenges in manufacturing engineered T cell therapies. *Int*
777 *Rev Immunol* [Internet]. 2022 [cited 2024 Jul 26];41(6):638. Available from:
778 </pmc/articles/PMC9815724/>
- 779 12. Castella M, Caballero-Baños M, Ortiz-Maldonado V, González-Navarro EA,
780 Suñé G, Antoñana-Vidósola A, et al. Point-of-care CAR T-cell production (ARI-

- 781 0001) using a closed semi-automatic bioreactor: Experience from an academic
782 phase i clinical trial. *Front Immunol* [Internet]. 2020 Mar 20 [cited 2024 May
783 9];11:500967. Available from: www.frontiersin.org
- 784 13. Lissandrello CA, Santos JA, Hsi P, Welch M, Mott VL, Kim ES, et al. High-
785 throughput continuous-flow microfluidic electroporation of mRNA into primary
786 human T cells for applications in cellular therapy manufacturing. *Sci Rep*
787 [Internet]. 2020 Dec 1 [cited 2021 Jun 12];10(1):18045. Available from:
788 <https://doi.org/10.1038/s41598-020-73755-0>
- 789 14. Louterback K, Bulur P, Dietz AB. Bioreactor on a chip: a microfluidic device
790 for closed production of human dendritic cells. *Cytotherapy* [Internet]. 2025 Jan
791 1 [cited 2025 Jun 26];27(1):121–7. Available from:
792 <https://www.sciencedirect.com/science/article/pii/S1465324924008375>
- 793 15. Moore N, Chevillet JR, Healey LJ, McBrine C, Doty D, Santos J, et al. A
794 Microfluidic Device to Enhance Viral Transduction Efficiency During
795 Manufacture of Engineered Cellular Therapies. *Sci Rep* [Internet]. 2019 Dec 1
796 [cited 2021 Jun 11];9(1):1–11. Available from: <https://doi.org/10.1038/s41598-019-50981-9>
- 798 16. Elsemary MT, Maritz MF, Smith LE, Warkiani M, Bandara V, Napoli S, et al.
799 Inertial Microfluidic Purification of CAR-T-Cell Products. *Adv Biol* [Internet].
800 2022 Jan 1 [cited 2025 Feb 12];6(1). Available from:
801 <https://pubmed.ncbi.nlm.nih.gov/34881810/>
- 802 17. Kim H, Kim S, Lim H, Chung AJ. Expanding CAR-T cell immunotherapy
803 horizons through microfluidics. *Lab Chip* [Internet]. 2024 Feb 27 [cited 2025
804 Jun 26];24(5):1088–120. Available from:
805 <https://pubs.rsc.org/en/content/articlehtml/2024/lc/d3lc00622k>
- 806 18. Wang Z, Kelley SO. Microfluidic technologies for enhancing the potency,
807 predictability and affordability of adoptive cell therapies. *Nat Biomed Eng.*
808 2025;
- 809 19. Sin WX, Jagannathan NS, Teo DBL, Kairi F, Fong SY, Tan JHL, et al. A high-
810 density microfluidic bioreactor for the automated manufacturing of CAR T cells.
811 *Nat Biomed Eng.* 2024 Dec 1;

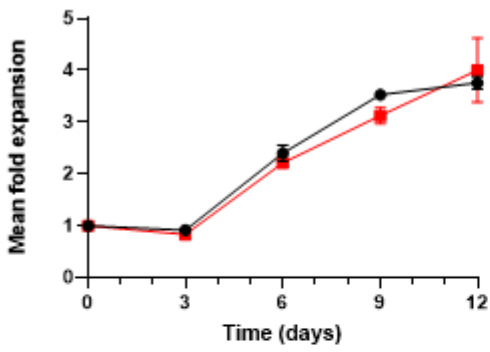
- 812 20. Noaks E, Peticone C, Kotsopoulou E, Bracewell DG. Enriching leukapheresis
813 improves T cell activation and transduction efficiency during CAR T
814 processing. *Mol Ther Methods Clin Dev*. 2021 Mar 12;20:675–87.
- 815 21. Havenga M, Hoogerbrugge P, Valerio D, Van Es HHG. Retroviral Stem Cell
816 Gene Therapy. *Stem Cells* [Internet]. 1997 May 1 [cited 2025 Feb
817 12];15(3):162–79. Available from:
818 <https://onlinelibrary.wiley.com/doi/full/10.1002/stem.150162>
- 819 22. Klasse PJ. Molecular Determinants of the Ratio of Inert to Infectious Virus
820 Particles. *Prog Mol Biol Transl Sci* [Internet]. 2014 [cited 2025 Feb
821 12];129:285. Available from:
822 <https://pmc.ncbi.nlm.nih.gov/articles/PMC4724431/>
- 823 23. Song S, Han M, Zhang H, Wang Y, Jiang H. Full screening and accurate
824 subtyping of HLA-A*02 alleles through group-specific amplification and mono-
825 allelic sequencing. *Cell Mol Immunol* [Internet]. 2013 Nov [cited 2024 May
826 8];10(6):490. Available from: </pmc/articles/PMC4002391/>
- 827 24. Cheon J, Kim S, Cheon J, Kim S. Intermediate layer-based bonding
828 techniques for polydimethylsiloxane/digital light processing 3D-printed
829 microfluidic devices. *JMiMi* [Internet]. 2019 Jul 1 [cited 2024 Jul
830 17];29(9):095005. Available from:
831 <https://ui.adsabs.harvard.edu/abs/2019JMiMi..29i5005C/abstract>
- 832 25. Fanelli G, Marks P, Aiyengar A, Romano M, Gooljar S, Kumar S, et al. Clinical
833 grade expansion protocol for the manufacture of thymus-derived Treg cells for
834 clinical application. *J Transl Med* [Internet]. 2025 Dec 1 [cited 2025 Jun
835 26];23(1):620. Available from:
836 <https://pmc.ncbi.nlm.nih.gov/articles/PMC12131477/>
- 837 26. Lemieszek MB, Findlay SD, Siegers GM. CellTrace™ Violet Flow Cytometric
838 Assay to Assess Cell Proliferation. *Methods Mol Biol* [Internet]. 2022 [cited
839 2024 Jul 17];2508:101–14. Available from:
840 <https://pubmed.ncbi.nlm.nih.gov/35737236/>

841

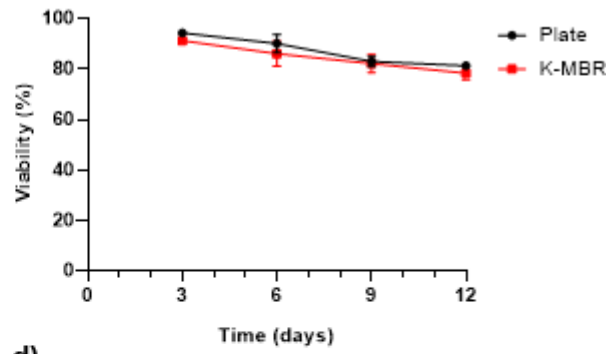
Journal Pre-proof



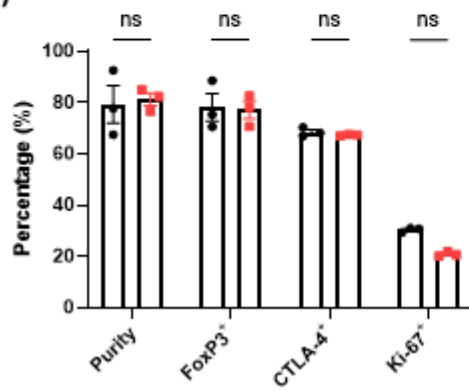
a)



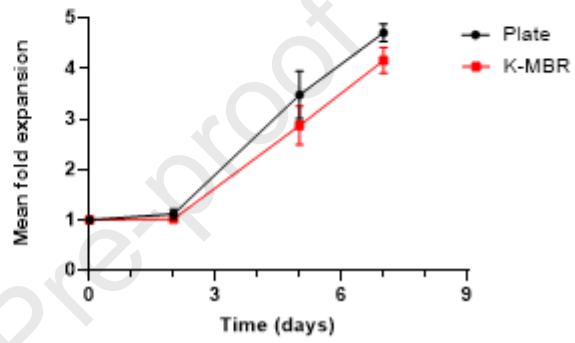
b)



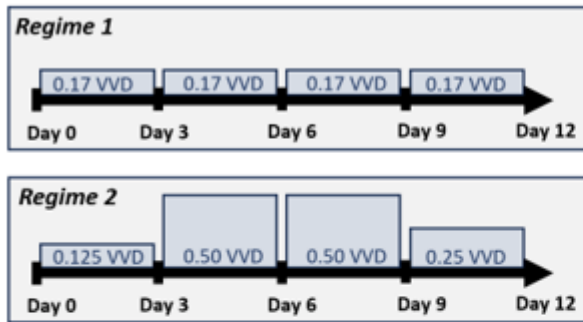
c)



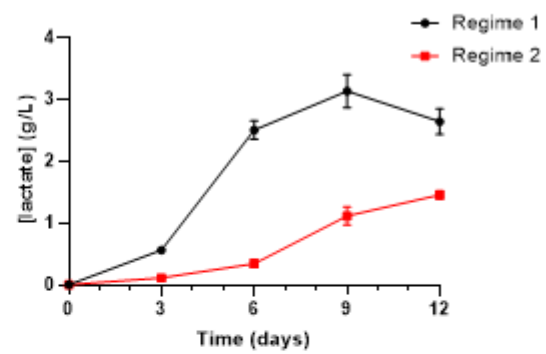
d)



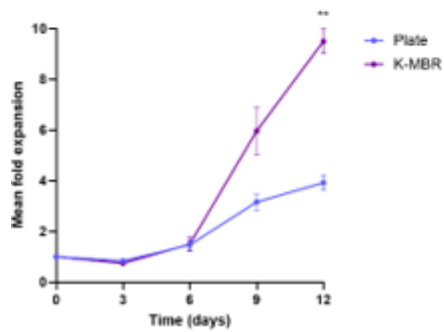
a)



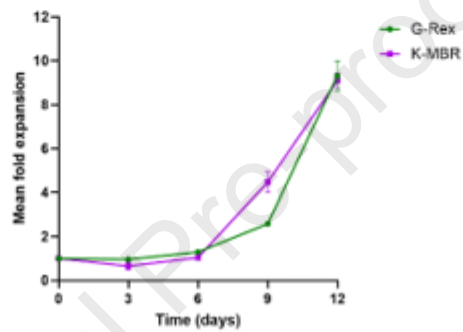
b)



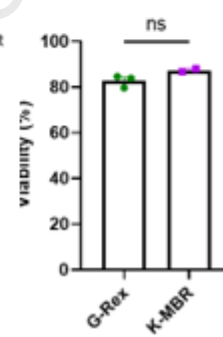
c)

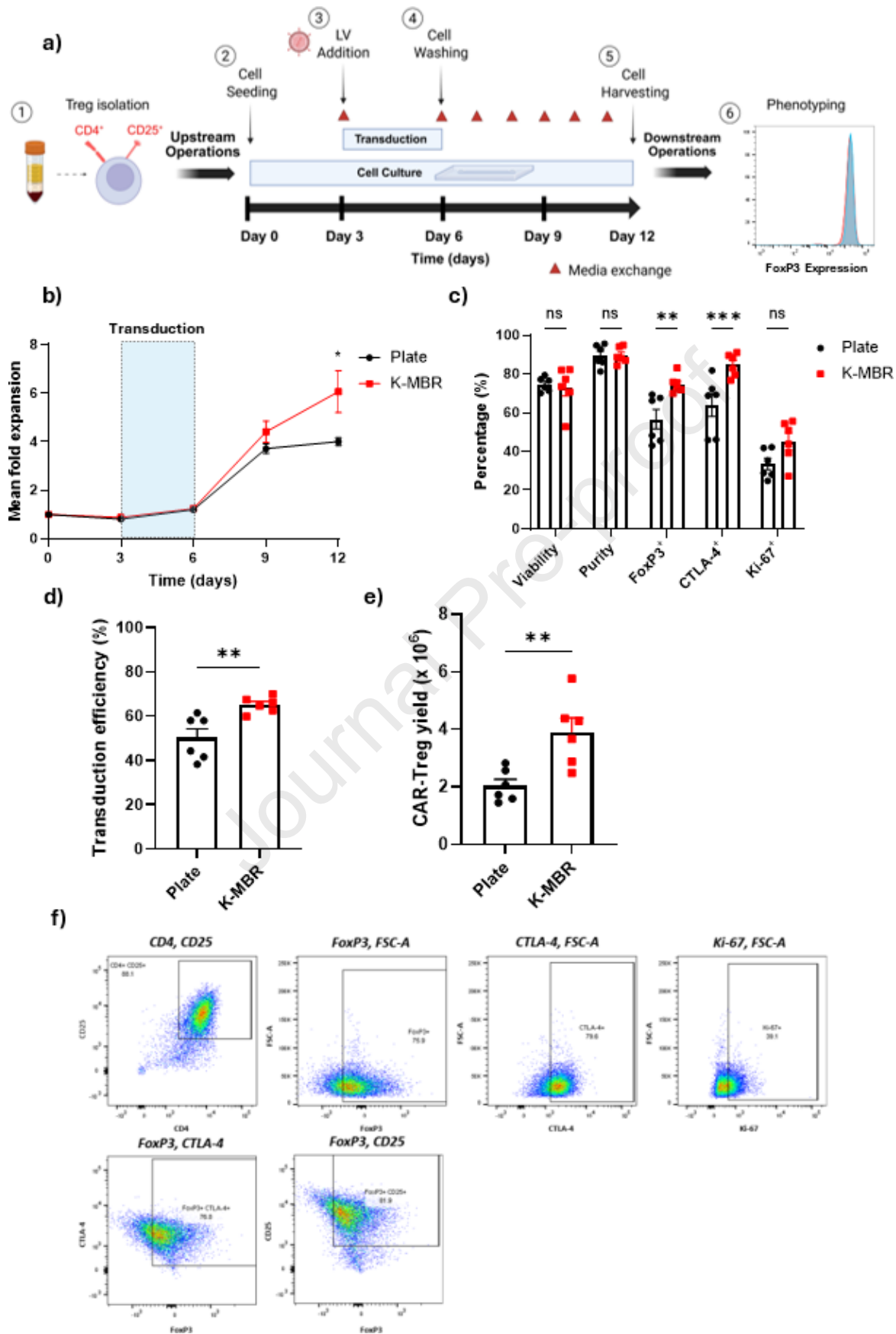


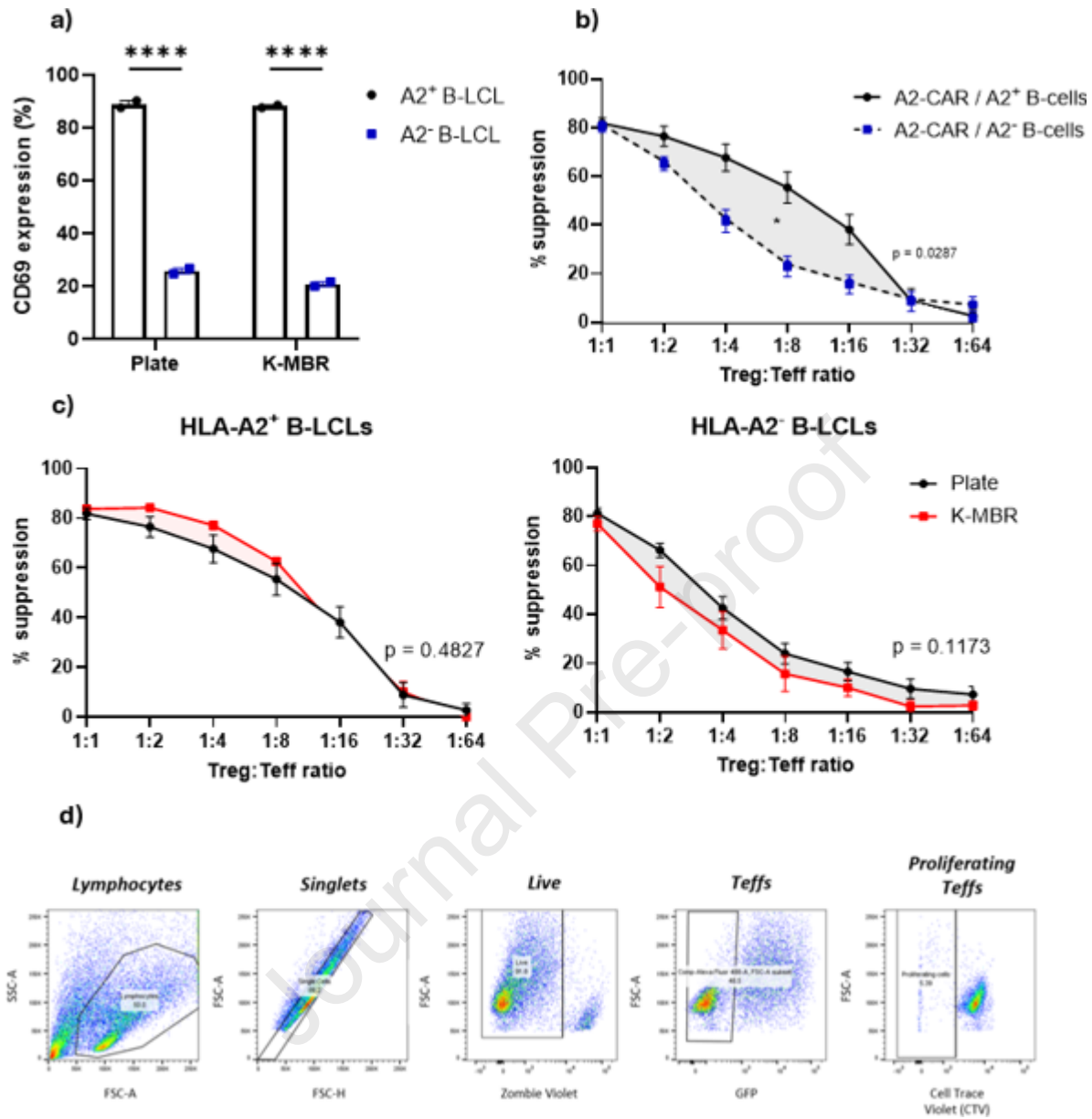
d)



e)









Journal Pre-proof

Highlights

- Perfusion microbioreactor achieves Treg expansion comparable to gold standard G-Rex device.
- Spatial confinement increases lentiviral transduction efficiency of primary, human cells.
- Compact, low-volume platform reduces the physical footprint of cell manufacturing.
- Device supports future automation and advances progress toward point-of-care production.

Key resources table

REAGENT or RESOURCE	SOURCE	IDENTIFIER
Antibodies		
Brilliant Violet 605™ anti-human CD4 Antibody (SK3)	Biolegend	Cat#344645
PE anti-human CD25 Antibody (BC96)	Biolegend	Cat#302605
PE/Cyanine7 anti-human CD69 Antibody (FN50)	Biolegend	Cat#310911
Brilliant Violet 785™ anti-human CD127 (IL-7R α) Antibody (A019D5)	Biolegend	Cat#351329
PE anti-human HLA-A2 Antibody (BB7.2)	Biolegend	Cat#343305
Alexa Fluor® 647 anti-human FOXP3 Antibody (206D)	Biolegend	Cat#320113
Brilliant Violet 510™ anti-human Ki-67 Antibody (11F6)	Biolegend	Cat#350517
PerCP/Cyanine5.5 anti-human CD152 (CTLA-4) Antibody (BNI3)	Biolegend	Cat#369607
Bacterial and virus strains		
HLA-A2 CAR second-generation pLNT/SSFV	Boardman et al. ³	N/A
Biological samples		
Peripheral blood leukocyte cones	NHSBT Tooting	Cat#NC24
Chemicals, peptides, and recombinant proteins		
CellTrace™ Violet Cell Proliferation Kit	ThermoFisher	Cat#C34557
Dynabeads™ Human T-Activator CD3/CD28	Gibco	Cat#11131D
T Cell TransAct™, human	Miltenyi	Cat#130-111-160
RosetteSep™ Human CD4+ T Cell Enrichment Cocktail	Stemcell	Cat#15062
Lymphoprep™	Stemcell	Cat#18060

CD25 MicroBeads II, human	Miltenyi	Cat#130-092-983
LS columns	Miltenyi	Cat#130-042-401
Recombinant Human IL-2 Protein	R&D Systems	Cat#202-IL
Rapamycin	LC Laboratories	Cat#R5000200M G
PEG-it™	System Biosciences	Cat#LV810A-1
LIVE/DEAD™ Fixable Near-IR Dead Cell Stain Kit	ThermoFisher	Cat#L34975
Critical commercial assays		
N/A	N/A	N/A
Deposited data		
N/A	N/A	N/A
Experimental models: Cell lines		
SPO (HLA-A2 ⁺ DR11 ⁺) B-LCLs	Boardman et al. ³	N/A
BM21 (HLA-A2 ⁻ DR11 ⁺) B-LCLs	Boardman et al. ³	N/A
Experimental models: Organisms/strains		
N/A	N/A	N/A
Oligonucleotides		
N/A	N/A	N/A
Recombinant DNA		
N/A	N/A	N/A
Software and algorithms		
FlowJo	FlowJo	https://www.flowjo.com/flowjo/download

Prism	GraphPad	https://www.graphpad.com/features
Leica LasX	Leica Microsystems	https://www.leica-microsystems.com/products/microscope-software/p/leica-las-x-ls/downloads/
Other		
N/A	N/A	N/A